Mathematical Modeling in Chronobiology

G. Bordyugov, P.O. Westermark, A. Korenčič, S. Bernard, and H. Herzel

Abstract Circadian clocks are autonomous oscillators entrained by external *Zeitgebers* such as light–dark and temperature cycles. On the cellular level, rhythms are generated by negative transcriptional feedback loops. In mammals, the suprachiasmatic nucleus (SCN) in the anterior part of the hypothalamus plays the role of the central circadian pacemaker. Coupling between individual neurons in the SCN leads to precise self-sustained oscillations even in the absence of external signals. These neuronal rhythms orchestrate the phasing of circadian oscillations in peripheral organs. Altogether, the mammalian circadian system can be regarded as a network of coupled oscillators. In order to understand the dynamic complexity of these rhythms, mathematical models successfully complement experimental investigations. Here we discuss basic ideas of modeling on three different levels (1) rhythm generation in single cells by delayed negative feedbacks, (2) synchronization of cells via external stimuli or cell–cell coupling, and (3) optimization of chronotherapy.

Keywords Bifurcations • Entrainment • Modelling • Oscillations • Synchronization

G. Bordyugov (✉) • H. Herzel
Institute for Theoretical Biology, Humboldt University, Invalidenstr. 43, 10115 Berlin, Germany
e-mail: Grigory.Bordyugov@hu-berlin.de; h.herzel@biologie.hu-berlin.de

P.O. Westermark
Institute for Theoretical Biology, Charité Universitätsmedizin, Invalidenstr. 43, 10115 Berlin, Germany

A. Korenčič
Institute of Biochemistry, Faculty of Medicine, University of Ljubljana, Vrazov trg 2, 1000 Ljubljana, Slovenia

S. Bernard
Institut Camille Jordan CNRS UMR5208, University Lyon 1, Equipe Dracula Team Inria, University of Lyon, Villeurbanne, 69622 Cedex, France

A. Kramer and M. Merrow (eds.), *Circadian Clocks*, Handbook of Experimental Pharmacology 217, DOI 10.1007/978-3-642-25950-0_14,

1 Introduction

The mammalian circadian clock can be regarded as a system of coupled oscillators. In virtually every cell, negative transcriptional feedback loops generate rhythm with a period of about 24 h (Zhang and Kay 2010; Minami et al. 2013; Buhr and Takahashi 2013). Circadian expression of hundreds of genes has been described in many tissues, including brain, liver, heart, and lung (Hastings et al. 2003; Keller et al. 2009; Brown and Azzi 2013). Even cultivated cells display pronounced rhythms upon stimulation (Balsalobre et al. 1998; Yagita and Okamura 2000) or temperature entrainment (Brown et al. 2002). As discussed elsewhere, the molecular clock orchestrates the timing of physiological and metabolic processes in our body (Hastings et al. 2003).

In mammals, the suprachiasmatic nucleus (SCN) is thought to play the role of the central circadian pacemaker. In the SCN, neurons are coupled via neurotransmitters and gap junctions (Welsh et al. 2010; Slat et al. 2013). The synchronization of neurons results in precise pacemaker rhythms which coordinate peripheral organs via neuronal and humoral signals. The phase of the SCN clock is entrained by external light–dark and temperature cycles. Feeding can serve as another potent *Zeitgeber*, which can entrain, for example, circadian rhythms in the liver (Stokkan et al. 2001). Circadian clock affects many physiological processes including cell division and detoxification. Consequently, the timing of therapeutic intervention can be optimized ("chronotherapy") (Lévi et al. 1997). The complexity of these processes has inspired systems biological approaches (Ukai and Ueda 2010). In particular, understanding the emergence of oscillations requires dynamical systems theory. Here, we discuss some aspects of mathematical modeling applied to circadian rhythms and chronotherapy.

Mathematical models of circadian rhythms have been applied on many levels (Pavlidis 1973; Winfree 1980; Daan and Berde 1978). Already decades ago, amplitude-phase models were developed to study entrainment properties, phase response properties, and seasonal variations (Wever 1965; Kronauer et al. 1982). Such models are still useful to study aspects of transients after jet lag (Granada and Herzel 2009), single cell oscillations (Westermark et al. 2009), effects of coupling (Bordyugov et al. 2011), and to optimize the phase response properties of circadian oscillators (Pfeuty et al. 2011). In the meantime, detailed biochemical models of the core clock have been developed (Leloup and Goldbeter 2003; Forger and Peskin 2003; Becker-Weimann et al. 2004). Such models describe transcriptional regulation, protein expression, posttranslational modifications, protein degradation, complex formation, and nuclear translocation (Relógio et al. 2011; Mirsky et al. 2009). However, quantitative details of many kinetic processes are not known and, thus, the choice of kinetic laws and parameters remains a major challenge. Simulations of coupled cells usually rely on simple cell models (Gonze et al. 2005). Recently, clock models have been connected to cell proliferation as an attempt to simulate chronotherapy (Lévi et al. 2008). Also theoretical attempts on describing systems with negative feedback and low numbers of molecules have proven the possibility of high-quality oscillations in such systems (Morelli and Jülicher 2007).

There is a statement that "all models are wrong, but some are useful" (George E. P. Box and Norman Richard Draper Wiley 1987). Indeed, mathematical models are cartoons of the overwhelming complexity of biological systems. Good models emphasize the most essential features of a system and reflect the major experimental facts. Model analysis can help to check the self-consistency of the modeling assumptions.

When the celebrated Hodgkin–Huxley model was established (Hodgkin and Huxley 1952), its theoretical analysis took as much effort as the experiments. Nowadays, computers are fast and cheap and computer simulations should complement expensive and time-consuming experiments. In many cases the development of mathematical models guides the design of appropriate quantitative measurements. In molecular chronobiology, models point to the role of transcriptional inhibition, degradation kinetics, and delays as discussed below. Mathematical models can systematically explore the role of feedback loops, the sensitivity to parameter variations and noise, and the efficacy of chronotherapies. Interesting theoretical predictions may stimulate novel experiments. Mathematical abstractions help to find common design principles of seemingly quite different biological systems. For example, most physiological oscillations are based on delayed negative feedback loops combined with cooperative interactions. Such cooperative interactions result, in turn, in a nonlinear response of the system to the feedback signal, which is required for generation of oscillations (Glass and Mackey 1988). Below we illustrate basic ideas of mathematical modeling in chronobiology using examples on different levels:

1. A simple oscillator model, which is based on a delayed negative feedback.
2. Synchronization of cells via external stimuli or cell–cell coupling.
3. Optimization of chronotherapy.

2 Oscillations Due to Delayed Negative Feedback

A large variety of physiological and biochemical oscillations has been modeled with the aid of delay differential equations (DDEs): Intracellular circadian rhythm generator (olde Scheper et al. 1999), drosophila endocycles (Zielke et al. 2011), periodic leukemia (Mackey and Glass 1977), Cheyne–Stokes respiration (Glass and Mackey 1988), blood pressure waves (Seidel and Herzel 1998), somite formation in zebra fish (Lewis 2003), circadian rhythms in *D. melanogaster* (Smolen et al. 2004), and mouse liver (Korenčič et al. 2012). Most detailed models of the mammalian clock are based on sets of ordinary differential equations (ODEs). In Appendix B, we show that DDEs and ODEs are intimately related. ODEs have been used to describe many details of the involved kinetic processes. DDEs have the advantage that fewer kinetic parameters are required. Equation (1) represents a simple DDE that can describe self-sustained oscillations:

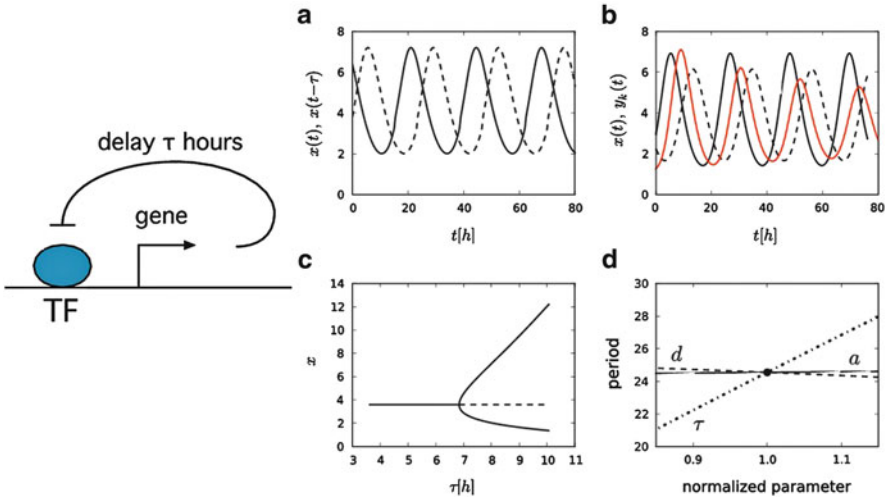

Fig. 1 *Left panel*: A sketch of a self-repressing gene regulation. Here τ denotes the time span between the transcription of the gene and its repression by its own gene products. TF represents an activating transcription factor such as BMAL1. *Right panel*: Results of simulation of Eq. (1). (**a**) A typical time course of oscillations in Eq. (1). The *solid line* denotes $x(t)$; the *dashed line* denotes the delayed variable $x(t-\tau)$. (**b**) Approximation of the DDE by an ODE system Eq. (11). *Black lines* correspond to chain length $k = 15$. The *solid black line* shows $x(k)$, and the *dashed black line* shows the time course of the last chain variable $y_{15}(t)$. The *red line* shows a decay of oscillations of $x(t)$ in Eq. (11) for chain length $k = 12$, which is not enough to successfully approximate oscillations in our DDE. (**c**) Bifurcation diagram for Eq. (1), showing a stable (the *horizontal solid line*) and unstable (*horizontal dashed line*) steady state for increasing delay τ. At $\tau \approx 7.0$ self-sustained oscillations emerge with maxima and minima shown by *solid lines*. (**d**) Dependence of oscillation period on the variation of the parameters normalized to their default values $a = 10.0$, $d = 0.2$, $\tau = 8.5$. The period is most strongly influenced by the delay τ (*dashed–dotted line*) and by the degradation rate d (*dashed line*)

$$\frac{\mathrm{d}x(t)}{\mathrm{d}t} = \frac{a}{1 + x^n(t-\tau)} - d \cdot x(t). \tag{1}$$

The dynamic variable $x(t)$ might represent a clock gene such as *Period2* whose protein product inhibits its own transcription after a delay τ (compare Fig. 1, left panel). The delay τ describes the time span between the transcription and the nuclear availability of the functional gene product. By introducing τ, we condense protein production, modification, complex formation, nuclear translocation, and epigenetic processes into a single parameter. Thus the model given by Eq. (1) is obviously a gross simplification, but it helps to understand the generation of self-sustained oscillations via delayed negative feedback loops (see Appendix A). The parameter a is the basal transcription rate, and d represents the degradation rate. A cooperativity index $n = 2$ can be justified since clock proteins frequently dimerize (Tyson et al. 1999; Bell-Pedersen et al. 2005).

For parameter values $a = 10.0$, $d = 0.2$ [a typical mRNA degradation rate (Schwanhäusser et al. 2011)], and $\tau = 8$, the model exhibits self-sustained oscillations (a "limit cycle") with a period of about 24 h. Figure 1a shows the corresponding oscillations of the state variable $x(t)$ and delayed version $x(t - \tau)$. The phase shift of 8 h resembles the phase shifts of mRNA and protein peaks of many clock genes (Reppert and Weaver 2001).

Figure 1b illustrates the close connection of DDE and ODEs. As shown in Appendix B, the explicit delay τ can be replaced by a chain of ODEs as in the widely used Goodwin model (Goodwin 1965; Griffith 1968; Ruoff et al. 2001). The corresponding auxiliary variables might represent different phosphorylation state complexes and nuclear translocation. For sufficiently long chains, ODEs approximate our DDE in Eq. (1) reasonably well.

In Appendix A, we provide a linear stability analysis of the steady state of Eq. (1). This approach allows the identification of the necessary conditions to get self-sustained oscillations. For small delays, the equilibrium is stable and perturbations decay exponentially. Intermediate delays lead to damped oscillations and further increase of τ leads to the onset of self-sustained oscillations. This transition has been termed "Hopf bifurcation" and is visualized in Fig. 1c.

The mathematical analysis in Appendix A provides further information on delayed feedback oscillators: the delay τ should be in the range of one-quarter to one-half of the period, and the inhibition should be sufficiently strong [fast decay of the transcription term in Eq. (1) with increasing "inhibitor" $x(t - \tau)$]. The period of the oscillation turns out to be nearly proportional to the delay τ.

Figure 1d displays the dependencies of the period on the model parameters τ, a, and d. As discussed above, the period grows linearly with the delay τ, whereas it decays slightly with increasing degradation parameter d. This is plausible since faster degradation implies shorter timescales of the mRNA dynamics and, hence, shorter periods. Variation of the basal transcription rate a has a minor effect on the period, consistent with Dibner et al. (2008). Extensive studies with more sophisticated models show that many insights obtained from our simple model given by Eq. (1) apply as well:

- Sufficiently strong nonlinearities are required to get self-sustained oscillations
- Overcritical delays of about a quarter to half of a period are necessary
- Delays and degradation rates have profound effects on the period

Transcriptional feedback loops with shorter-than-circadian periodicity including Hes1 (Hirata et al. 2002), p53 (Lahav et al. 2004), and NFκB (Nelson et al. 2004; Hoffmann and Baltimore 2006) have smaller delays, which result in shorter periods of a few hours. In circadian clocks, the particularly long delay is necessary to get 24 h rhythms. The central role of delays and degradation rate has been demonstrated by the intensively studied Familial Advanced Sleep Phase Syndrome (FASPS) (Vanselow et al. 2006).

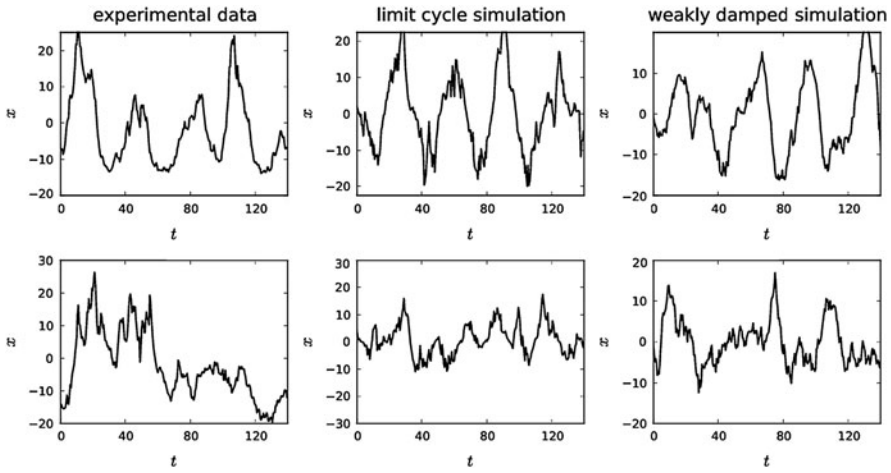

Fig. 2 Two representative bioluminescence time series from dispersed SCN neurons (*left column*). The *middle column* shows simulations of the corresponding limit cycle model (see Eq. (2)) with added noise. Similar simulations are obtained with weakly damped noise-induced oscillations (*right column*). The model parameters were estimated from the time courses in the *left-most column* as explained in (Westermark et al. 2009). This implies that the two models are tailored to the specific cells

3 Precision via Synchronization and Entrainment

On the organismic level, circadian clocks are astonishingly precise (Enright 1980; Herzog et al. 2004). Even in constant darkness (DD), the behaviorial activity onset varies from day to day by a few minutes only (Oster et al. 2002). In contrast, circadian rhythms in single cells are much noisier (Welsh et al. 1995; Liu et al. 2007), and thus for single cells, stochastic (i.e., accounting for fluctuations) models are necessary. Fitting amplitude-phase models to single cells resulted in broad distributions of estimated model parameters (Westermark et al. 2009). For example, single cell periods were found to obey a Gaussian distribution with a standard deviation of about 1.5 h (Welsh et al. 1995; Honma et al. 2004; Herzog et al. 2004). In this section, we illustrate how external signals and intercellular coupling can lead to precise circadian oscillations despite noise on the single cell scale.

We analyzed several hundred single cell recordings of circadian rhythms. The first column of Fig. 2 displays time courses of two selected cells. The upper one clearly shows periodicity, whereas the lower one is quite noisy. We have shown that such single cell data can be represented by noise-driven amplitude-phase models (Westermark et al. 2009). Interestingly, two types of fits were successful: single cell circadian time series could be modeled either by limit cycle models or as weakly damped oscillators. The examples in Fig. 2 illustrates that both types of simulations seem reasonable.

The model for self-sustained oscillations is given in polar coordinates by

$$\frac{\mathrm{d}r_i}{\mathrm{d}t} = -\lambda_i(r_i - A_i),$$
$$\frac{\mathrm{d}\varphi_i}{\mathrm{d}t} = \frac{2\pi}{\tau_i}, \quad i = 1, 2, \ldots, N. \tag{2}$$

The variable r_i is the radial coordinate, and φ_i is the phase of the i-th cell. The parameter A_i corresponds to the amplitude of the self-sustained oscillations. The parameter λ_i is the amplitude relaxation rate. Small values of λ_i result in slow amplitude relaxation towards the amplitude A_i. In order to simulate the intrinsic stochasticity of the single cell rhythms (Raser and O'Shea 2005; Raj and van Oudenaarden 2008), we added random noise to Eq. (2) (Westermark et al. 2009). Details of the simulation procedure are explained in Appendix C. Weakly damped oscillators are described by Eq. (2) with vanishing amplitudes A_i. In this way single cell rhythms can be quantified by a handful of parameters, including estimated periods τ_i and the relaxation rates λ_i.

Figure 3 shows histograms of parameters estimated from 140 dispersed SCN neurons from wild-type mice (Liu et al. 2007). The limit cycle model (left) and the damped oscillator model (right) lead to a wide range of single cell periods as reported earlier (Welsh et al. 1995; Honma et al. 2004; Herzog et al. 2004). The estimated relaxation times differ considerably between two models. Damped oscillator models exhibit smaller values of λ_i, which results in longer relaxation times. Due to slow relaxation, random perturbations can induce fairly regular noise-induced oscillations (Ebeling et al. 1983; Ko et al. 2010). Long relaxation times [or, equivalently, high oscillator qualities Q (Westermark et al. 2009)] lead to resonant behavior.

Below we discuss the response of simulated oscillators to a short pulse, external time-periodic forcing, and intercellular coupling. As parameter values, we take the direct estimates from 140 dispersed SCN neurons. We compare simulations with self-sustained oscillators and weakly damped noise-driven oscillators.

In cultivated cells, stimuli such as fresh serum, forskolin, dexamethasone, or temperature pulses can induce temporarily synchronized rhythms (Balsalobre et al. 1998; Yagita and Okamura 2000). After the stimuli are ceased, however, the synchrony is lost within a few cycles and the averaged signal damps out. This decay is caused by single cell damping and dephasing of cells due to different periods.

In Fig. 4 we compare the response of simulated cells to short pulses. For both limit cycle and weakly damped models, we observed the expected damped rhythms of the population mean. Single cells were found to exhibit much larger amplitudes than the average signal. Due to the longer relaxation time, damped oscillators (Fig. 4, right panel) show larger amplitudes and the damped oscillations persist a few more cycles. This supports our expectation that weakly damped oscillators are good "resonators." By looking only at the averaged signal (Fig. 4, time series in thick black lines), it is difficult to distinguish between limit cycle and weakly

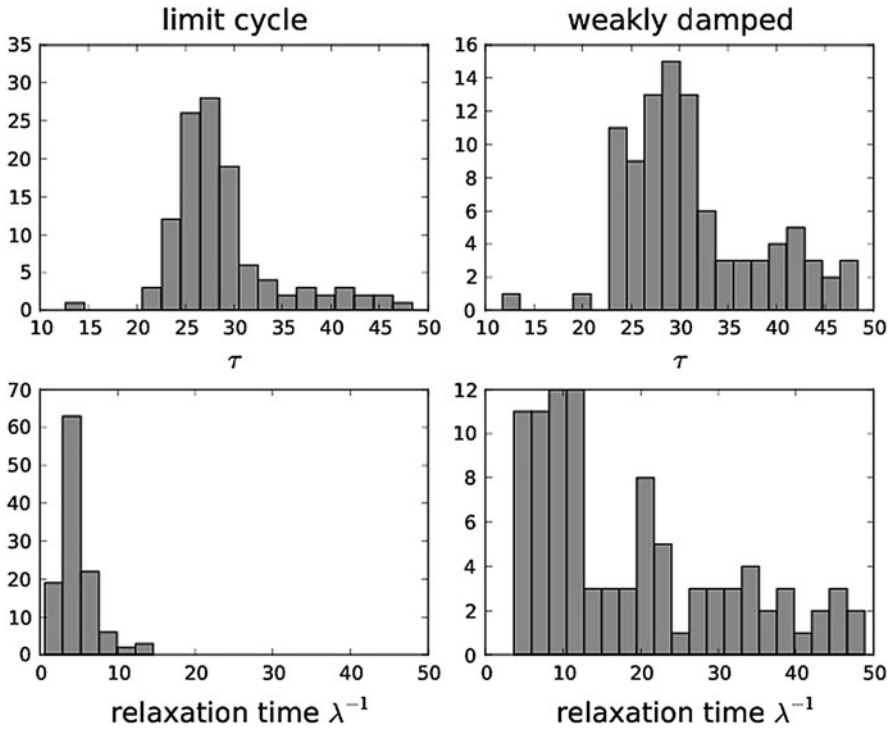

Fig. 3 Histograms of parameters estimated from a total of 140 SCN neurons. The *left column* refers to the limit cycle model (see Eq. (2)), showing a peak at circadian periods and relatively fast relaxation to their amplitudes A_i. Fitted parameters of damped oscillators (*right column*) exhibit longer relaxation times λ^{-1}, thus allowing noise-induced oscillations as shown in Fig. 2, *upper right panel*

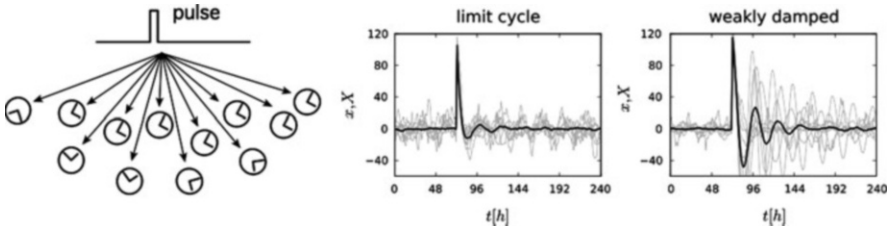

Fig. 4 Temporary synchronization of simulated cells via a pulse-like perturbation. Selected cells are visualized in *gray*. *Left panel*: Cartoon visualizing a pulse acting on oscillators. *Central panel*: Ensemble of noisy limit cycle oscillators. *Right panel*: Ensemble of noisy damped oscillators. In both time series, the *thick black line* represents the averaged signal. Parameters were extracted from experimental time series (Liu et al. 2007; Westermark et al. 2009)

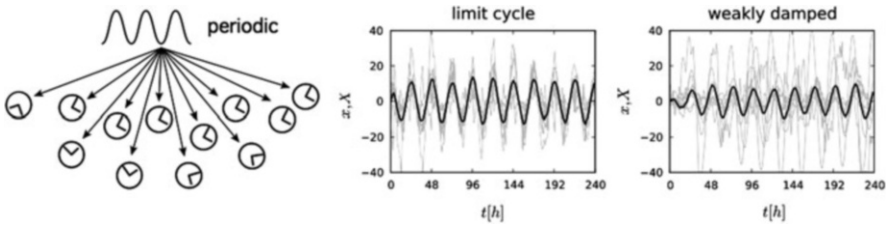

Fig. 5 Synchronization of simulated single cell oscillators by an external time-periodic *Zeitgeber* (see also Appendix C). *Left panel*: Cartoon visualizing a common periodic *Zeitgeber* acting on oscillators. *Central panel*: The averaged signal indicates that precise rhythms can be established in an ensemble of self-sustained oscillators and for weakly damped oscillators (*right panel*)

damped models. Thus, the characterization of single cell properties requires careful, long-lasting single cell experiments (Nagoshi et al. 2004; Liu et al. 2007) or resonance experiments as suggested in (Westermark et al. 2009). Such resonance experiments might be performed using temperature entrainment (Brown et al. 2002; Buhr et al. 2010). Recent studies have shown that periodic warm–cold cycles can synchronize peripheral tissues such as lung (Abraham et al. 2010) or epidermal cells (Spörl et al. 2010).

Figure 5 shows simulations of temperature entrainment. We find that relatively weak external signals can lead to fairly precise rhythms of the average signal (time series in thick black lines in Fig. 5), even though single cells are still quite noisy (time series in thin gray lines in Fig. 5). Both self-sustained oscillators (Fig. 5, central panel) and weakly damped oscillators (Fig. 5, right panel) lead to regular averaged oscillations. Some damped oscillators have relatively long relaxation time λ_i^{-1} (see Fig. 3, lower right graph), which results in large amplitudes due to stronger resonance. The distribution of the periods τ_i is however wide (see upper left plot in Fig. 3) and thus the average signal is weaker compared to the entrained self-sustained oscillator.

So far we simulated uncoupled cells synchronized via external signals. SCN neurons are coupled via gap junctions (Long et al. 2005) and neurotransmitters such as VIP (Aton et al. 2005). Such coupling leads to precise and robust SCN rhythms relatively insensitive to temperature signals (Buhr et al. 2010; Abraham et al. 2010). The periodic secretion of neurotransmitters induces a common oscillatory level, which we model by a periodic mean field, see Appendix C. Figure 6 demonstrates that such mean-field coupling can easily synchronize ensembles of noisy single cell oscillators. The coupling via mean field in Fig. 6 again leads to a pronounced amplitude expansion since a distributed neurotransmitter acts as periodic driving signal.

There is an ongoing debate whether dispersed single cells can be regarded as self-sustained oscillators or weakly damped oscillators (Nagoshi et al. 2004; Gonze et al. 2005; Westermark et al. 2009). Webb et al. (2009) find a mixture of seemingly self-sustained and damped cells the SCN. Our simulations of pulses in Fig. 4, of entrainment in Fig. 5, and of synchronization in Fig. 6 indicate that both model

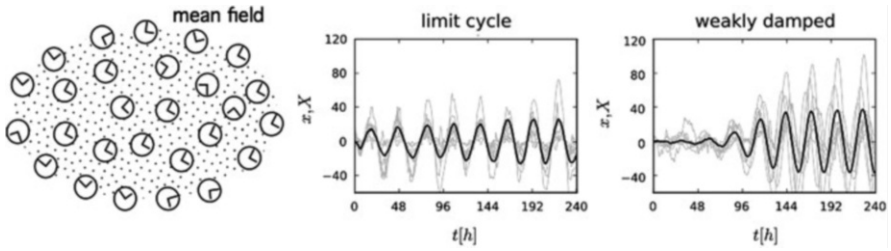

Fig. 6 Synchronization of single cell oscillators coupled through a common mean-field (*black dots* in the background of the *left panel*) as described in Appendix C. Within a few cycles coupling can induce synchrony in an ensemble of self-sustained oscillators (*central panel*) and in a set of damped oscillators (*right panel*). Single cell time-series (*thin gray lines* in the time series) reveal that selected cells exhibit quite large amplitudes due to resonance with the oscillating mean field

types can reproduce gross features of experimental observations. Consequently, long-lasting single cell recordings are needed to extract the characteristics of the oscillators. In addition, controlled resonance experiments will be helpful for determining parameters of single cell rhythms.

4 Modeling Chronotherapy

Circadian timing modifies efficacy and toxicity of many drugs (Lévi and Schibler 2007; Ortiz-Tudela et al. 2013; Musiek and FitzGerald 2013). In particular, the tolerability and efficacy of anticancer agents depend on treatment timing (Mormont and Levi 2003; Lévi et al. 1997). In mice experiments, it has been shown that a 4-h difference of drug delivery time can change the survival rate from 20 % to 80 % (Gorbacheva et al. 2005). Mathematical models of chronomodulated administration schedules ("chronotherapy") complement experiments and clinical studies (Hrushesky et al. 1989; Basdevant et al. 2005; Ballesta et al. 2011; Ortiz-Tudela et al. 2013).

Comprehensive mathematical modeling of chronotherapy should incorporate the pharmacokinetics and -dynamics (PK/PD) of drugs (Derendorf and Meibohm 1999) and the interaction of circadian rhythms and proliferation (Hunt and Sassone-Corsi 2007). Even though PK/PD models and cell cycle models (Chauhan et al. 2011) are available, the comprehensive mathematical description of chronotherapy remains an attractive challenge. Here we report the core results of recently published simulations (Bernard et al. 2010) with simple cell cycle models under periodic circadian modulation. The model is useful to study the efficacy of chronotherapeutic treatment of fast and slow growing cancer cell populations. Mathematical modeling allows simulation of various temporal treatment schedules. The central output of the model is the therapeutic index which takes into account the removal of cancer cells together with the quantification of the side-effects (Bernard et al. 2010).

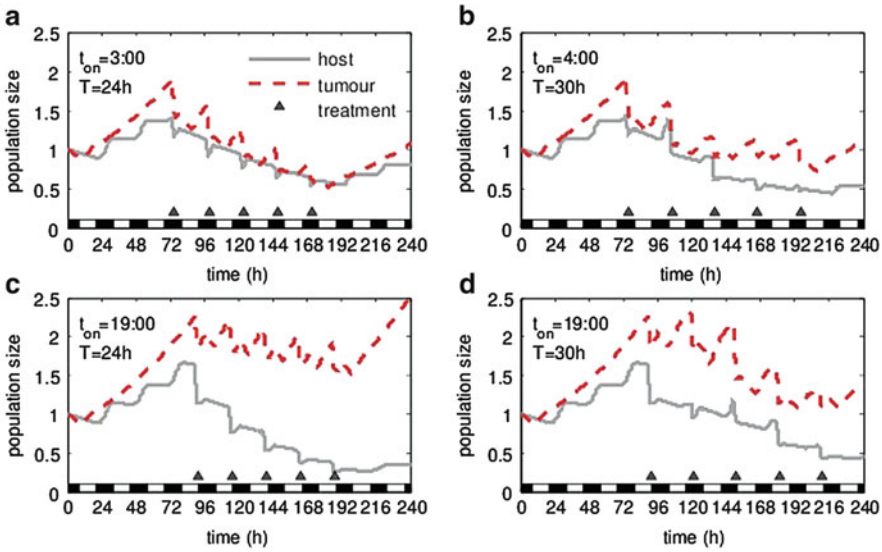

Fig. 7 Visualization of chronotherapy simulations at 24 h intervals (*left*) and 30 h intervals (*right*). The *triangles* represent treatment, *dashed lines* represent tumor growth, and *solid gray lines* host cells. The *upper graphs* show treatment at the optimal phase, whereas the *lower graphs* display the worst phases for both treatment schedules

The left graphs of Fig. 7 demonstrate the application of drugs at two different phases of a 24 h cycle. The optimal phase (Fig. 7a) and the worst phase (Fig. 7c) are compared. The simulations reproduce the experimental findings (Gorbacheva et al. 2005) that drug delivery at wrong phase can result in undesirable effects, in particular, in fast growing tumors (see Bernard et al. (2010) for details). A possible explanation for that is a resonance between the time-periodic therapy and circadian clock (Andersen and Mackey 2001). Such a resonance can be avoided by therapies with a different period. Patients often carry programmable portable pumps, and hence periods of, e.g., 30 h can be easily realized clinically. The simulation in Fig. 7d demonstrates that the 30-h-periodic treatment is successful even for the worst phase. Since it is difficult to measure the phase of circadian rhythm in a clinical situation, a treatment schedule that is applicable at any phase seems quite promising.

5 Discussion

Unfortunately, comprehensive and precise models of the mammalian circadian clock are not at the horizon. Quantitative details of many essential molecular processes such as complex formation, posttranslational modification, proteasomal

degradation, and transcriptional regulation are not available. Nevertheless, mathematical models can provide some insights into the design principles of circadian rhythms.

As shown above, simple models of delayed negative feedback loops point to the role of overcritical (i.e., beyond a certain critical value) delays and nonlinearities. For the circadian clock, there must be a minimal delay of 6 h between transcription of clock genes and their inhibition. This result emphasizes the importance of controlled degradation and nuclear translocation associated with phosphorylation and complex formation.

For many purposes traditional amplitude-phase models remain useful. For instance, phase response properties, entrainment range, and effects of coupling can be addressed with such simplified models. We have shown that temporary synchronization via pulses, entrainment, and resonance phenomena can be reproduced using amplitude-phase models with experimentally validated parameters (Westermark et al. 2009). These simulations reveal that ensembles of weakly damped single cell oscillators can constitute precise clocks thanks to coupling. This observation points to an unsolved question: How many SCN cells are in vivo truly self-sustained oscillators (Webb et al. 2009)?

In the context of optimizing chronotherapy, we simulated the interaction of circadian rhythms with cell proliferation and drug delivery. Even if many details including PK/PD were neglected, a plausible conclusion could be drawn: Due to strong resonance effects, a 24 h therapy might be more risky than other therapeutic cycles such as 30 h treatments. Of course, our minimal models have to be complemented by more detailed studies such as Ballesta et al. (2011). There are many more exciting questions that can be approached using mathematical models:

- What might be the role of auxiliary feedback loops in the core clock machinery?
- How are harmonics in gene expression profiles generated?
- How are entrainment phases controlled across seasons?
- What might be the function of the SCN heterogeneity?
- How do circadian clock, metabolism, immune response, and detoxification interact?
- What are the major selective advantages of a functioning circadian clock?

In order to address these intriguing questions, appropriate theoretical studies can successfully complement experimental approaches.

Acknowledgments The authors thank Jana Hinners and Anna Erzberger for their contributions to numerical simulations, Adrian E. Granada, Michael Mackey, and Francis Levi for fruitful discussions, and DFG (SFB 618, InKomBio) and BMBF (ColoNet, Circage FKZ 0315899) for financial support.

Appendix A: Oscillations Due to Delayed Negative Feedback

A.1 The Model

One of the simplest models for a self-suppressing gene reads

$$\frac{\mathrm{d}x(t)}{\mathrm{d}t} = \frac{a}{1 + bx^n(t-\tau)} - d\,x(t). \tag{3}$$

Here, the time-dependent state variable $x(t)$ corresponds to the mRNA level of a clock gene, for instance, *Per2* at time t. The positive parameter d is the mRNA degradation rate, large values correspond to a rapid degradation, whereas small values model more stable mRNAs. Parameter a determines the basal transcription rate in the absence of the inhibitor.

The self-inhibition is modeled in the following way: For simplicity, we consciously refrain from modeling all intermediate steps, which lead from the mRNA to its protein product translocated back into the nucleus. We merely postulate that the nuclear protein abundance is proportional with the factor b to the amount of mRNA τ hours earlier. The power n is the cooperativity index, which in the case of dimerization is given by $n = 2$. The self-inhibition is reflected by the delayed state variable $x(t - \tau)$ appearing in the denominator. Its high values decrease the net production rate of the mRNA $\mathrm{d}x(t)/\mathrm{d}t$. Asymptotically, for very large values of $x(t - \tau)$, the production rate of mRNA tends to zero.

A typical choice of parameters is given by the following values: The basal transcription rate can be set to $a = 1$, because we have arbitrary units, the degradation rate to $d = 0.2\ \mathrm{h}^{-1}$, which corresponds to a typical mRNA half-life (Sharova et al. 2009), and the time delay to $\tau = 8$ h, which is a characteristic delay between *Per2* and phosphorylated nuclear PER2.

We stress that the model given by Eq. (3) is qualitative and we do not expect an exact quantitative correspondence of its predictions with the numerical values from experiments. However, many features of the oscillations can be predicted by the model equation. For example, parameter ranges of the delay τ and the degradation rate can be determined that allow the generation of oscillations.

A.2 Steady State and Its Stability

We generalize our model given by Eq. (1) to a one-dimensional DDE as follows:

$$\frac{\mathrm{d}x(t)}{\mathrm{d}t} = g(x(t-\tau)) - d \cdot x(t), \tag{4}$$

where τ is a time delay, $g(\cdot)$ is a nonlinear function, and $d > 0$ is a degradation constant. An example is the nonlinear feedback in the form of

$$g(x) = \frac{a}{1 + bx^n}, \tag{5}$$

with the parameters a, b, n as discussed above.

A steady state of Eq. (4) satisfy $\frac{\mathrm{d}x(t)}{\mathrm{d}t} = 0$ and is given by the nonlinear equation

$$g(x) - dx = 0,$$

which is in the case of Eq. (5) equivalent to

$$a - d(1 + bx^n)x = 0. \tag{6}$$

This is a nonlinear equation, which can be analytically solved only for small values of the exponent n. Generally, for arbitrary n, the steady state can be determined numerically.

Suppose that we have solved the steady state equation and the equilibrium is given by $x = x_0$. We are now interested in the question of the stability of x_0: that is, whether the system in the course of time will return back to equilibrium x_0 or depart from it. For this purpose, we introduce the ansatz

$$x(t) = x_0 + y(t), \tag{7}$$

with a small function of time $y(t)$, which is the deviation of $x(t)$ from its steady state value x_0. In order to determine the stability of x_0, we need to see, whether the derivation, $y(t)$, would grow or decay in time. We emphasize that we are interested in what happens in the intermediate neighborhood of x_0, which implies that $y(t)$ is small.

Let us introduce our ansatz into the equations. We have for the left-hand side of Eq. (4)

$$\frac{\mathrm{d}x(t)}{\mathrm{d}t} = \frac{\mathrm{d}y(t)}{\mathrm{d}t}$$

and correspondingly for its right-hand side by using a Taylor expansion up to the first order:

$$\begin{aligned} g(x(t-\tau)) - dx(t) &= g(x_0 + y(t-\tau)) - dx_0 - dy(t) \approx \\ &\approx g(x_0) + Jy(t-\tau) - dx_0 - dy(t) = \\ &= Jy(t-\tau) - dy(t). \end{aligned}$$

Here, J is the slope of the nonlinear function g in the steady state x_0 given by

$$J = \frac{\mathrm{d}}{\mathrm{d}x} g(x_0).$$

Putting both sides together results in

$$\frac{\mathrm{d}y(t)}{\mathrm{d}t} = Jy(t-\tau) - dy(t). \tag{8}$$

This is a DDE for the unknown function $y(t)$. This equation is linear, and we can solve it by an exponential ansatz

$$y(t) = y_0 \mathrm{e}^{\lambda t},$$

with the unknown complex number λ. The last ansatz, when substituted in Eq. (8), leads to

$$y_0 \lambda \mathrm{e}^{\lambda t} = J y_0 \mathrm{e}^{\lambda(t-\tau)} - d y_0 \mathrm{e}^{\lambda t},$$

and after dividing by $y_0 \mathrm{e}^{\lambda t}$ it results in the transcendental characteristic equation for λ:

$$\lambda = J\mathrm{e}^{-\lambda\tau} - d. \tag{9}$$

If we find a value λ which solves Eq. (9), the function $y(t) = y_0 \mathrm{e}^{\lambda t}$ would be a solution to Eq. (8). The growth or decay of $y(t) = y_0 \mathrm{e}^{\lambda t}$ is determined by the sign of the real part of λ. If Re $\lambda < 0$, the function $y(t)$ will decay in the course of time, which would correspond to a stable steady state x_0. If Re $\lambda > 0$, the function $y(t)$ grows, which means that the system departs from steady state x_0 and the latter is unstable.

To sum up, given steady state x_0, we have to solve Eq. (9) for the unknown λ, whose real part determines the stability of x_0. Note that Eq. (9) depends on the steady state x_0 through J, on the value of the time delay τ, and on the degradation rate d. Thus we expect that the stability of the steady state can be changed by tuning any of those parameters.

A.3 Oscillation Onset (Hopf Bifurcation)

Here, we are interested in a special situation, where the complex exponent λ has a zero real part. This corresponds to a parameter set, for which the stability of the steady state changes: if we change one of the parameters slightly, the real part will become nonzero and the steady state would either loose or gain stability, depending on the direction of the parameter change.

We introduce $\lambda = \mu + \mathrm{i}\omega$, which, when substituted in Eq. (9), results in

$$\mu = J\mathrm{e}^{-\mu\tau}\cos(\omega\tau) - d,$$
$$\omega = -J\mathrm{e}^{-\mu\tau}\sin(\omega\tau).$$

We are interested in the situation when $\mu = 0$, since it is associated with a change of stability of the steady state. At the same time when the steady state looses its stability, a small limit cycle emerges from the steady state. The period T of this limit cycle is close to $2\pi/\omega$. This scenario is known as a Hopf bifurcation. Going on with our calculations, the condition $\mu = 0$ simplifies the above two equations to

$$J\cos(\omega\tau) - d = 0,$$
$$-J\sin(\omega\tau) = \omega.$$

Using $\cos^2(\omega\tau) + \sin^2(\omega\tau) = 1$, we have

$$J^2 = d^2 + \omega^2,$$

and $d = \sqrt{J^2 - \omega^2}$. This in turn leads to the expression for the critical value of delay:

$$\cos(\omega\tau) = \frac{\sqrt{J^2 - \omega^2}}{J} = \sqrt{1 - \frac{\omega^2}{J^2}}.$$

Moreover, we can express $\omega = \sqrt{J^2 - d^2}$ and have $\cos(\omega\tau) = d/J$, which gives the value for the critical delay

$$\tau = \frac{\arccos(d/J)}{\omega} = \frac{\arccos(d/J)}{\sqrt{J^2 - d^2}}.$$

We can analyze this equation a bit further: Owing to $d \geq 0$ and $J < 0$, d/J is negative or zero. Hence, $\arccos(d/J)$ assumes values in between $\pi/2$ (corresponding to $d/J = 0$) and π (corresponding to $d/J = -1$). Thus, the value of τ is in between $2\pi/\omega$ and π/ω, which is exactly one-fourth to one-half of $T = 2\pi/\omega$. Here, T approximates the period of the limit cycle, which emerges from the steady state in a Hopf bifurcation with $\lambda = 0 + \mathrm{i}\omega$.

Our analytical calculations allowed us to specify the parameters where a Hopf bifurcation occurs: From $J = \sqrt{d^2 + \omega^2}$ we see that a certain slope is needed. Furthermore, the delay must exceed a quarter of a period (6 h for circadian rhythms). Finally, the period is approximately proportional to the delay.

Appendix B: Explicit Delays Versus Reaction Chains

In the main text we studied the DDE

$$\frac{\mathrm{d}x(t)}{\mathrm{d}t} = g(x(t-\tau)) - d \cdot x(t). \tag{10}$$

If $x(t)$ represents the mRNA of a clock gene, the transcriptional inhibition is executed by its time-delayed value $x(t-\tau)$. In reality, the mRNA is spliced, exported, and translated to a protein. The protein forms complexes, can be posttranslationally modified, and will be translocated to the nucleus, where it regulates transcription. This series of events can be modeled in principle by studying all the corresponding intermediate concentrations and the resulting inhibitory complex. Since many quantitative details are not known, we introduced here the shortcut with an explicit delay.

It turns out that variables with explicit delays can be approximated by a chain of k intermediate auxiliary variables $y_i(t)$:

$$\begin{aligned}
\frac{\mathrm{d}x(t)}{\mathrm{d}t} &= g(y_k(t)) - dx(t),\\
\frac{\mathrm{d}y_1(t)}{\mathrm{d}t} &= h(x(t) - y_1(t)),\\
\frac{\mathrm{d}y_2(t)}{\mathrm{d}t} &= h(y_1(t) - y_2(t)),\\
&\cdots\\
\frac{\mathrm{d}y_k(t)}{\mathrm{d}t} &= h(y_{k-1}(t) - y_k(t)).
\end{aligned} \tag{11}$$

If we choose $h = k/\tau$, the chain of ODEs approximates the DDE (10) [this transformation is called the *linear chain trick* (MacDonald et al. 2008; Smith 2010)]. Here we sketch a short explanation for that claim.

We begin by *ad hoc* introducing a family of gamma functions $G_{h,q}$ by

$$G_{h,q}(t) = \frac{h^q t^{q-1} \mathrm{e}^{-ht}}{(q-1)!}.$$

A first useful observation is that the time derivative of the gamma functions satisfies the following relation

$$\frac{\mathrm{d}}{\mathrm{d}t} G_{h,q}(t) = h(G_{h,q-1}(t) - G_{h,q}(t)), \quad q = 2, 3, \ldots, k,$$

which formally reminds the last k equations in (11). Using this result, a straightforward differentiation shows that functions, $y_q(t)$, given by the convolution integrals,

$$y_q(t) = \int_{-\infty}^{t} x(s) G_{h,q}(t-s)\mathrm{d}s, \quad q = 1, 2, \ldots, k, \tag{12}$$

indeed solve the last k equations in (11).

We now turn to the properties of $y_k(t)$. It is formed by convolution integrals of $x(t)$ with the gamma function $G_{h,k}(t)$. These functions have mean value at $t = k/h$ and variance proportional to k. Thus, for large k, the functions $G_{h,k}(t)$ become narrower, approximating a peak centered at k/h.

In the above integral (12) for $q = k$, we aim at localizing $x(s)$ at the time moment $t - \tau$ by properly choosing $G_{h,k}(t - s)$. The condition $s = t - \tau$ results in $G_{h,k}(t - s) = G_{h,k}(\tau)$. By an appropriate choice of parameter h, we tune the gamma function in such a way that its mean value is at the delayed time point $t - \tau$. Owing that the mean value of $G_{h,k}(\tau)$ is at $\tau = k/h$, this leads to the sought condition for h: $h = k/\tau$. We conclude that the solution of the last equation of system (11), given by

$$y_k(t) = \int_{-\infty}^{t} x(s) G_{h,k}(t - s)\, \mathrm{d}s$$

with $h = k/\tau$ indeed approximates the delayed value of x: $y_k(t) \approx x(t - \tau)$. The approximation becomes better for larger chain lengths due to narrower $G_{h,k}$ for large k.

These calculations illustrate that chains of ODEs as studied in most clock models are closely related to DDEs analyzed above. The fact that long chains (i.e., large number k of the ODE equations) lead to sharper delays could be related to the observation that many posttranslational modifications (Vanselow et al. 2006), complex formations (Zhang et al. 2009; Robles et al. 2010), and epigenetic modification (Bellet and Sassone-Corsi 2010) are involved in generation of 24 h rhythms. We also refer to Forger (2011) for a somewhat similar study of the Goodwin model as a chain of three interconnected steps.

Appendix C: Modeling Details of Single Cell Oscillators

The dynamics of single cells was described either by a noisy limit cycle model or a noise-driven weakly damped oscillator model. For N cells, the governing deterministic differential equations read:

$$\begin{aligned} \frac{\mathrm{d}r_i}{\mathrm{d}t} &= -\lambda_i (r_i - A_i), \\ \frac{\mathrm{d}\varphi_i}{\mathrm{d}t} &= \frac{2\pi}{\tau_i}, \quad i = 1, 2, \ldots, N. \end{aligned} \tag{13}$$

Here, λ_i is the radial relaxation rate, τ_i is the cell's period, and A_i is the cell's signal amplitude. All three parameters were estimated from experimental data as explained in (Westermark et al. 2009). Limit cycle oscillators have a nonzero amplitude A_i, whereas for damped oscillators we set $A_i = 0$. The cell stochasticity

was modeled by Gaussian noise sources added to the right-hand sides of Eq. (13). The variances of the noise terms were also estimated from experimental data as in (Westermark et al. 2009). For time integration of the resulting stochastic differential equation, we used the Euler–Murayama method.

For both limit cycle oscillators and weakly damped ones, three simulation protocols were realized.

- Synchronization by a pulse: At a certain time moment, we simultaneously shifted each oscillator in a specific direction by 120 dimensionless units (see Fig. 4).
- External periodic forcing: For the results presented in Fig. 5, we subjected oscillators to an external periodic force with a 24 h period and an amplitude of 0.5 dimensionless units. This driving force is much smaller than the typical oscillator amplitude of 10–20 (dimensionless units).
- Synchronization via mean field: In the third protocol (see Fig. 6), the oscillators were subjected to the mean field Z, which resulted from averaging across the ensemble:

$$Z = \frac{1}{N} \sum_{N} r_i e^{i\varphi_i}.$$

For linear damped oscillators, a saturation of the mean field at 20 dimensionless units was introduced in order to avoid amplitude explosion due to the linearity of the model.

References

Abraham U, Granada AE, Westermark PO, Heine M, Kramer A, Herzel H (2010) Coupling governs entrainment range of circadian clocks. Mol Syst Biol 6:438

Andersen L, Mackey M (2001) Resonance in periodic chemotherapy: a case study of acute myelogenous leukemia. J Theor Biol 209:113–130

Aton S, Colwell C, Harmar A, Waschek J, Herzog E (2005) Vasoactive intestinal polypeptide mediates circadian rhythmicity and synchrony in mammalian clock neurons. Nat Neurosci 8:476–483

Ballesta A, Dulong S, Abbara C, Cohen B, Okyar A, Clairambault J, Levi F (2011) A combined experimental and mathematical approach for molecular-based optimization of irinotecan circadian delivery. PLoS Comput Biol 7:e1002143

Balsalobre A, Damiola F, Schibler U (1998) A serum shock induces circadian gene expression in mammalian tissue culture cells. Cell 93:929–937

Basdevant C, Clairambault J, Lévi F (2005) Optimisation of time-scheduled regimen for anti-cancer drug infusion. ESAIM Math Model Numer Anal 39:1069–1086

Becker-Weimann S, Wolf J, Herzel H, Kramer A (2004) Modeling feedback loops of the mammalian circadian oscillator. Biophys J 87:3023–3034

Bellet M, Sassone-Corsi P (2010) Mammalian circadian clock and metabolism–the epigenetic link. J Cell Sci 123:3837–3848

Bell-Pedersen D, Cassone V, Earnest D, Golden S, Hardin P, Thomas T, Zoran M (2005) Circadian rhythms from multiple oscillators: lessons from diverse organisms. Nat Rev Genet 6:544–556

Bernard S, Bernard B, Lévi F, Herzel H (2010) Tumor growth rate determines the timing of optimal chronomodulated treatment schedules. PLoS Comput Biol 6:e1000712

Bordyugov G, Granada A, Herzel H (2011) How coupling determines the entrainment of circadian clocks. Eur Phys J B 82:227–234

Brown SA, Azzi A (2013) Peripheral circadian oscillators in mammals. In: Kramer A, Merrow M (eds) Circadian clocks, vol 217, Handbook of experimental pharmacology. Springer, Heidelberg

Brown S, Zumbrunn G, Fleury-Olela F, Preitner N, Schibler U (2002) Rhythms of mammalian body temperature can sustain peripheral circadian clocks. Curr Biol 12:1574–1583

Buhr ED, Takahashi JS (2013) Molecular components of the mammalian circadian clock. In: Kramer A, Merrow M (eds) Circadian clocks, vol 217, Handbook of experimental pharmacology. Springer, Heidelberg

Buhr ED, Yoo SH, Takahashi JS (2010) Temperature as a universal resetting cue for mammalian circadian oscillators. Science 330:379–385

Chauhan A, Lorenzen S, Herzel H, Bernard S (2011) Regulation of mammalian cell cycle progression in the regenerating liver. J Theor Biol 283:103–112

Daan S, Berde C (1978) Two coupled oscillators: simulations of the circadian pacemaker in mammalian activity rhythms. J Theor Biol 70:297–313

Derendorf H, Meibohm B (1999) Modeling of pharmacokinetic/pharmacodynamic (PK/PD) relationships: concepts and perspectives. Pharm Res 16:176–185

Dibner C, Sage D, Unser M, Bauer C, d'Eysmond T, Naef F, Schibler U (2008) Circadian gene expression is resilient to large fluctuations in overall transcription rates. EMBO J 28:123–134

Ebeling W, Herzel H, Selkov EE (1983) The influence of noise on an oscillating glycolytic model. Studia Biophysica 98:147–154

Enright J (1980) Temporal precision in circadian systems: a reliable neuronal clock from unreliable components? Science 209:1542–1545

Forger D (2011) Signal processing in cellular clocks. Proc Natl Acad Sci 108:4281–4285

Forger DB, Peskin CS (2003) A detailed predictive model of the mammalian circadian clock. Proc Natl Acad Sci USA 100:14806–14811

George E. P. Box and Norman Richard Draper Wiley (1987) Robustness in the strategy of scientific model building. Technical report, Defence Technical Information Center Document

Glass L, Mackey M (1988) From clocks to chaos: the rhythms of life. University Press, Princeton, NJ

Gonze D, Bernard S, Waltermann C, Kramer A, Herzel H (2005) Spontaneous synchronization of coupled circadian oscillators. Biophys J 89:120–129

Goodwin B (1965) Oscillatory behavior in enzymatic control processes. Adv Enzyme Regul 3:425–428

Gorbacheva V, Kondratov R, Zhang R, Cherukuri S, Gudkov A, Takahashi J, Antoch M (2005) Circadian sensitivity to the chemotherapeutic agent cyclophosphamide depends on the functional status of the CLOCK/BMAL1 transactivation complex. Proc Natl Acad Sci USA 102:3407–3412

Granada AE, Herzel H (2009) How to achieve fast entrainment? The timescale to synchronization. PLoS One 4:e7057

Griffith J (1968) Mathematics of cellular control processes. I: Negative feedback to one gene. J Theor Biol 20:202–208

Hastings M, Reddy A, Maywood E et al (2003) A clockwork web: circadian timing in brain and periphery, in health and disease. Nat Rev Neurosci 4:649–661

Herzog ED, Aton SJ, Numano R, Sakaki Y, Tei H (2004) Temporal precision in the mammalian circadian system: a reliable clock from less reliable neurons. J Biol Rhythms 19:35–46

Hirata H, Yoshiura S, Ohtsuka T, Bessho Y, Harada T, Yoshikawa K, Kageyama R (2002) Oscillatory expression of the bHLH factor Hes1 regulated by a negative feedback loop. Science 298:840–843

Hodgkin A, Huxley A (1952) A quantitative description of membrane current and its application to conduction and excitation in nerve. J Physiol 117:500–544

Hoffmann A, Baltimore D (2006) Circuitry of nuclear factor κB signaling. Immunol Rev 210:171–186

Honma S, Nakamura W, Shirakawa T, Honma K (2004) Diversity in the circadian periods of single neurons of the rat suprachiasmatic nucleus depends on nuclear structure and intrinsic period. Neurosci Lett 358:173–176

Hrushesky W, Von Roemeling R, Sothern R (1989) Circadian chronotherapy: from animal experiments to human cancer chemotherapy. In: Lemmer B (ed) Chronopharamacology: cellular and biochemical interactions, vol 720. Marcel Dekker, New York, pp 439–473

Hunt T, Sassone-Corsi P (2007) Riding tandem: circadian clocks and the cell cycle. Cell 129:461–464

Keller M, Mazuch J, Abraham U, Eom G, Herzog E, Volk H, Kramer A, Maier B (2009) A circadian clock in macrophages controls inflammatory immune responses. Proc Natl Acad Sci USA 106:21407–21412

Ko C, Yamada Y, Welsh D, Buhr E, Liu A, Zhang E, Ralph M, Kay S, Forger D, Takahashi J (2010) Emergence of noise-induced oscillations in the central circadian pacemaker. PLoS Biol 8:e1000513

Korenčič A, Bordyugov G, Košir R, Rozman D, Goličik M, Herzel H (2012) The interplay of *cis*-regulator elements rules circadian rhythms in mouse liver. PLoS One 7(11):e0046835

Kronauer RE, Czeisler CA, Pilato SF, Moore-Ede MC, Weitzman ED (1982) Mathematical model of the human circadian system with two interacting oscillators. Am J Physiol 242:R3–17

Lahav G, Rosenfeld N, Sigal A, Geva-Zatorsky N, Levine A, Elowitz M, Alon U (2004) Dynamics of the p53-Mdm2 feedback loop in individual cells. Nat Genet 36:147–150

Leloup JC, Goldbeter A (2003) Toward a detailed computational model for the mammalian circadian clock. Proc Natl Acad Sci USA 100:7051–7056

Lévi F, Schibler U (2007) Circadian rhythms: mechanisms and therapeutic implications. Annu Rev Pharmacol Toxicol 47:593–628

Lévi F, Zidani R, Misset J et al (1997) Randomised multicentre trial of chronotherapy with oxaliplatin, fluorouracil, and folinic acid in metastatic colorectal cancer. Lancet 350:681–686

Lévi F, Altinok A, Clairambault J, Goldbeter A (2008) Implications of circadian clocks for the rhythmic delivery of cancer therapeutics. Philos Trans R Soc A 366:3575–3598

Lewis J (2003) Autoinhibition with transcriptional delay: a simple mechanism for the zebrafish somitogenesis oscillator. Curr Biol 13:1398–1408

Liu AC, Welsh DK, Ko CH, Tran HG, Zhang EE, Priest AA, Buhr ED, Singer O, Meeker K, Verma IM, Doyle FJ, Takahashi JS, Kay SA (2007) Intercellular coupling confers robustness against mutations in the SCN circadian clock network. Cell 129:605–616

Long M, Jutras M, Connors B, Burwell R (2005) Electrical synapses coordinate activity in the suprachiasmatic nucleus. Nat Neurosci 8:61–66

MacDonald N, Cannings C, Hoppensteadt F (2008) Biological delay systems: linear stability theory. University Press, Cambridge, MA

Mackey M, Glass L (1977) Oscillation and chaos in physiological control systems. Science 197:287–289

Minami Y, Ode KL, Ueda HR (2013) Mammalian circadian clock; the roles of transcriptional repression and delay. In: Kramer A, Merrow M (eds) Circadian clocks, vol 217, Handbook of experimental pharmacology. Springer, Heidelberg

Mirsky H, Liu A, Welsh D, Kay S, Doyle F (2009) A model of the cell-autonomous mammalian circadian clock. Proc Natl Acad Sci 106:11107–11112

Morelli LG, Jülicher F (2007) Precision of genetic oscillators and clocks. Phys Rev Lett 98:228101

Mormont M, Levi F (2003) Cancer chronotherapy: principles, applications, and perspectives. Cancer 97:155–169

Musiek ES, FitzGerald GA (2013) Molecular clocks in pharmacology. In: Kramer A, Merrow M (eds) Circadian clocks, vol 217, Handbook of experimental pharmacology. Springer, Heidelberg

Nagoshi E, Saini C, Bauer C, Laroche T, Naef F, Schibler U (2004) Circadian gene expression in individual fibroblasts: cell-autonomous and self-sustained oscillators pass time to daughter cells. Cell 119:693–705

Nelson D, Ihekwaba A, Elliott M, Johnson J, Gibney C, Foreman B, Nelson G, See V, Horton C, Spiller D et al (2004) Oscillations in NF-κB signaling control the dynamics of gene expression. Science 306:704–708

olde Scheper T, Klinkenberg D, Pennartz C, van Pelt J et al (1999) A mathematical model for the intracellular circadian rhythm generator. J Neurosci 19:40–47

Ortiz-Tudela E, Mteyrek A, Ballesta A, Innominato PF, Lévi F (2013) Cancer chronotherapeutics: experimental, theoretical and clinical aspects. In: Kramer A, Merrow M (eds) Circadian clocks, vol 217, Handbook of experimental pharmacology. Springer, Heidelberg

Oster H, Yasui A, Van Der Horst G, Albrecht U (2002) Disruption of mCry2 restores circadian rhythmicity in mPer2 mutant mice. Genes Dev 16:2633–2638

Pavlidis T (1973) Biological oscillators: their mathematical analysis. Academic, Waltham, MA

Pfeuty B, Thommen Q, Lefranc M (2011) Robust entrainment of circadian oscillators requires specific phase response curves. Biophys J 100:2557–2565

Raj A, van Oudenaarden A (2008) Nature, nurture, or chance: stochastic gene expression and its consequences. Cell 135:216–226

Raser J, O'Shea E (2005) Noise in gene expression: origins, consequences, and control. Science 309:2010–2013

Relógio A, Westermark P, Wallach T, Schellenberg K, Kramer A, Herzel H (2011) Tuning the mammalian circadian clock: robust synergy of two loops. PLoS Comput Biol 7:e1002309

Reppert S, Weaver D (2001) Molecular analysis of mammalian circadian rhythms. Annu Rev Physiol 63:647–676

Robles M, Boyault C, Knutti D, Padmanabhan K, Weitz C (2010) Identification of RACK1 and protein kinase Cα as integral components of the mammalian circadian clock. Science 327:463–466

Ruoff P, Vinsjevik M, Monnerjahn C, Rensing L (2001) The Goodwin model: simulating the effect of light pulses on the circadian sporulation rhythm of Neurospora crassa. J Theor Biol 209:29–42

Schwanhäusser B, Busse D, Li N, Dittmar G, Schuchhardt J, Wolf J, Chen W, Selbach M (2011) Global quantification of mammalian gene expression control. Nature 473:337–342

Seidel H, Herzel H (1998) Bifurcations in a nonlinear model of the baroreceptor-cardiac reflex. Physica D 115:145–160

Sharova LV, Sharov AA, Nedorezov T, Piao Y, Shaik N, Ko MSH (2009) Database for mRNA half-life of 19 977 genes obtained by DNA microarray analysis of pluripotent and differentiating mouse embryonic stem cells. DNA Res 16:45–58

Slat E, Freeman GM, Herzog ED (2013) The clock in the brain: neurons, glia and networks in daily rhythms. In: Kramer A, Merrow M (eds) Circadian clocks, vol 217, Handbook of experimental pharmacology. Springer, Heidelberg

Smith H (2010) An introduction to delay differential equations with applications to the life sciences. Springer, Heidelberg

Smolen P, Hardin P, Lo B, Baxter D, Byrne J (2004) Simulation of Drosophila circadian oscillations, mutations, and light responses by a model with VRI, PDP-1, and CLK. Biophys J 86:2786–2802

Spörl F, Schellenberg K, Blatt T, Wenck H, Wittern K, Schrader A, Kramer A (2010) A circadian clock in HaCaT keratinocytes. J Invest Dermatol 131:338–348

Stokkan K, Yamazaki S, Tei H, Sakaki Y, Menaker M (2001) Entrainment of the circadian clock in the liver by feeding. Science 291:490–439

Tyson J, Hong C, Thron CD, Novak B (1999) A simple model of circadian rhythms based on dimerization and proteolysis of PER and TIM. Biophys J 77:2411–2417

Ukai H, Ueda HR (2010) Systems biology of mammalian circadian clocks. Annu Rev Physiol 72:579–603

Vanselow K, Vanselow JT, Westermark PO, Reischl S, Maier B, Korte T, Herrmann A, Herzel H, Schlosser A, Kramer A (2006) Differential effects of PER2 phosphorylation: molecular basis for the human familial advanced sleep phase syndrome (FASPS). Genes Dev 20:2660–2672

Webb A, Angelo N, Huettner J, Herzog E (2009) Intrinsic, nondeterministic circadian rhythm generation in identified mammalian neurons. Proc Natl Acad Sci USA 106:16493–16498

Welsh DK, Logothetis DE, Meister M, Reppert SM (1995) Individual neurons dissociated from rat suprachiasmatic nucleus express independently phased circadian firing rhythms. Neuron 14:697–706

Welsh DK, Takahashi JS, Kay SA (2010) Suprachiasmatic nucleus: cell autonomy and network properties. Annu Rev Physiol 72:551–577

Westermark PO, Welsh DK, Okamura H, Herzel H (2009) Quantification of circadian rhythms in single cells. PLoS Comput Biol 5:e1000580

Wever R (1965) A mathematical model for circadian rhythms. Circadian Clocks 47:47–63

Winfree A (1980) The geometry of biological time. Springer, New York

Yagita K, Okamura H (2000) Forskolin induces circadian gene expression of rPer1, rPer2 and dbp in mammalian rat-1 fibroblasts. FEBS Lett 465:79–82

Zhang EE, Kay SA (2010) Clocks not winding down: unravelling circadian networks. Nat Rev Mol Cell Biol 11:764–776

Zhang E, Liu A, Hirota T, Miraglia L, Welch G, Pongsawakul P, Liu X, Atwood A, Huss J III, Janes J et al (2009) A genome-wide RNAi screen for modifiers of the circadian clock in human cells. Cell 139:199–210

Zielke N, Kim K, Tran V, Shibutani S, Bravo M, Nagarajan S, van Straaten M, Woods B, von Dassow G, Rottig C et al (2011) Control of Drosophila endocycles by E2F and CRL4CDT2. Nature 480:123–127